Development 133, 517-528 doi:10.1242/dev.02228

The Sonic hedgehog pathway independently controls the patterning, proliferation and survival of neuroepithelial cells by regulating Gli activity

Jordi Cayuso[1], Fausto Ulloa[2], Barny Cox[2], James Briscoe[2,*] and Elisa Martí[1,*]

During CNS development, the proliferation of progenitors must be coordinated with the pattern of neuronal subtype generation. In the ventral neural tube, Sonic hedgehog acts as a long range morphogen to organise the pattern of cell differentiation by controlling the activity of Gli transcription factors. Here, we provide evidence that the same pathway also acts directly at long range to promote the proliferation and survival of progenitor cells. Blockade of Shh signaling or inhibition of Gli activity results in cell autonomous decreases in progenitor proliferation and survival. Conversely, positive Gli activity promotes proliferation and rescues the effects of inhibiting Shh signaling. Analysis of neural cells indicates that Shh/Gli signaling regulates the G1 phase of cell cycle and the expression of the anti-apoptotic factor Bcl2. Furthermore, Shh signaling independently regulates patterning, proliferation and survival of neural cells, thus Shh/Gli activity couples these separate cellular responses of progenitors to coordinate neural development.

KEY WORDS: Spinal cord, Neural development, Pattern formation, Cell proliferation, Cell survival, Hedgehog signaling, Gli proteins, Chick

INTRODUCTION

The early embryonic vertebrate neural tube is composed of proliferating progenitors and terminally differentiating neurons distributed in a characteristic arrangement. Mitotically active cells form a pseudostratified epithelium that occupies the medially located ventricular zone. As cells differentiate in this progenitor region, they exit the cell cycle and migrate in a medial to lateral direction to form a mantle zone of postmitotic neurons (Ramón y Cajal, 1911). Distinct neuronal subtypes emerge in a precise spatial order from progenitor cells, resulting in the partition of the dorsoventral axis of the neural tube into discrete regions occupied by different neuronal subtypes (Jessell, 2000). At the same time, a balance between differentiation and proliferation of progenitors ensures the growth of the neural tube and replenishes the pool of progenitors, allowing continued rounds of neuronal and glial differentiation.

Much attention has focused on the mechanisms that control the identity of differentiating neurons. Particularly well characterized is the regulation of neuronal subtype identity in caudal regions of the neural tube that comprise the spinal cord and hindbrain. In ventral regions, Sonic hedgehog (Shh) secreted from the floor plate and notochord acts as a long-range graded signal that controls the pattern of neurogenesis (Jessell, 2000; Briscoe and Ericson, 2001). Dorsally, members of the Bmp and Wnt families of signaling molecules expressed by the roof plate and overlying ectoderm have been implicated in determining neuronal subtype identity (Helms and Johnson, 2003). These signals act by regulating the spatial pattern of expression, in progenitor cells, of transcription factors that include members of the homeodomain protein (HD) and basic helix-loop-helix (bHLH) families (Helms and Johnson, 2003; Briscoe et al., 2000; Ericson et al., 1997; Muhr et al., 2001; Novitch et al., 2001; Pierani et al., 2001; Vallstedt et al., 2001) and the experimental evidence indicates that changing the progenitor transcription factor code alters neuronal subtype in a predictable manner. Thus, the profile of transcription factor expression, established by the secreted signals, determines the subtype identity of the neurons generated from a progenitor cell (Briscoe et al., 2000).

Less well understood is how the growth and proliferation of progenitors in the neural tube is controlled and how this is coordinated with the mechanisms that control the pattern of neurogenesis. A number of studies have suggested an important role for Wnt signaling in promoting the proliferation and survival of neural progenitors at least in dorsal regions of the caudal neural tube (Dickinson et al., 1994; Megason and McMahon, 2002; Panhuysen et al., 2004). However, increasing experimental data supports the idea that Shh may also play a major role. The development of a number of anterior neural structures, including the cerebellum (Dahmane and Ruiz i Altaba, 1999; Pons et al., 2001; Wallace, 1999; Wechsler-Reya and Scott, 1999), neocortex and tectum (Dahmane et al., 2001; Palma and Ruiz i Altaba, 2004) depends on a mitogenic response to Shh signaling; moreover, Shh signaling is also required for the maintenance of neural stem cells during late development and in adult CNS (Lai et al., 2003; Machold et al., 2003). In caudal regions, notochord removal causes a decrease in the size of the neural tube (Charrier et al., 2001; van Straaten and Hekking, 1991) and notochord-derived signals can regulate neuroepithelial cell proliferation (van Straaten et al., 1989; Placzek et al., 1993). Consistent with the idea that this signal corresponds to Shh, the ectopic expression of Shh (Rowitch et al., 1999) or the ectopic activation of the Shh signaling pathway (Goodrich et al., 1997; Epstein et al., 1996; Hynes et al., 2000) results in hyper-proliferation of progenitors. Furthermore, genetic manipulation of the dose of two endogenous inhibitors of the pathway, Patched1 and Hip1, results in a noticeable and dose-dependent enlargement of the neural tube (Jeong and McMahon, 2005). Conversely, blockade of Shh signaling either by the genetic removal of Shh or components of the Shh

[1]Instituto de Biología Molecular de Barcelona, CSIC, Parc Científic de Barcelona, C/Josep Samitier 1-5, Barcelona, Spain. [2]National Institute for Medical Research, The Ridgeway, Mill Hill, London NW71AA, UK.

*Authors for correspondence (e-mail: emgbmc@ibmb.csic.es; james.briscoe@nimr.mrc.ac.uk)

Accepted 29 November 2005

pathway (Chiang et al., 1996; Litingtung and Chiang, 2000; Wijgerde et al., 2002) results in a decrease in both the proliferation and survival of progenitor cells within the neuroepithelium.

Shh signals by binding its receptor Patched (Ptc), a multi-pass transmembrane protein. In the absence of Shh, Ptc acts to suppress the activity of a second transmembrane protein, Smoothened (Smo) (for a review, see Lum and Beachy, 2004). Liganding of Ptc by Shh relieves repression of Smo, then, through a mechanism yet to be fully elucidated, Smo signals intracellularly to zinc-finger-containing transcription factors of the Gli family – highly conserved transcriptional mediators of the Shh pathway that can activate or repress transcription of specific target genes (reviewed by Jacob and Briscoe, 2003). Despite evidence of the role for Shh in regulating the survival and proliferation of progenitors in the neural tube, how Shh mediates these activities remained unclear. Here, by manipulating components of the Shh signaling pathway in vivo in chick embryos, we provide evidence that Shh acts directly on progenitor cells to promote neural progenitor proliferation and survival. Moreover, our data indicate that the regulation of Gli activity by Shh signaling is responsible for controlling progenitor proliferation and survival. Finally, we provide evidence that the Shh regulated patterning, proliferation and survival of progenitors are separable activities, suggesting that each of these cellular properties is an independently regulated response to Shh/Gli signaling. Thus, Shh signaling appears to coordinate directly the growth and patterning of developing neural tube through Gli mediated transcriptional regulation of discrete sets of target genes.

MATERIALS AND METHODS

Constructs

A deleted form of mouse patched lacking the second large extracellular loop ($Ptc1\Delta^{loop2}$) (Briscoe et al., 2001), a deleted form of human Gli3 encoding amino acids 1-768 (Gli3R) (Persson et al., 2002), the complementary deleted form of human Gli3 encoding amino acids 468-1580 ($Gli3A^{HIGH}$) (Stamataki et al., 2005), the sequence encoding amino acids 471-645 of the human Gli3 zinc-finger (Gli-ZnF) and a dominant negative form of protein kinase A (dnPKA) (Epstein et al., 1996) were all inserted into pCIG (Megason and McMahon, 2002) upstream of an internal ribosomal entry site (IRES) and three nuclear localization sequences tagged EGFP in pCAGGS expression vector (Niwa et al., 1991). A human *BCL2*-coding sequence inserted into pcDNA3 expression vector was used for co-electroporation.

Chick in ovo electroporation

Eggs from White-Leghorn chickens were incubated at 38.5°C in an atmosphere of 70% humidity. Embryos were staged according to Hamburger and Hamilton (HH) (Hamburger and Hamilton, 1951).

Chick embryos were electroporated with Clontech purified plasmid DNA at 2-3 μg/μl in H_2O with 50 ng/ml Fast Green. Briefly, plasmid DNA was injected into the lumen of HH stage 10-12 neural tubes, electrodes were placed either side of the neural tube and electroporation carried out using and Intracel Dual Pulse (TSS10) electroporator delivering five 50 msecond square pulses of 30-40 V.

Transfected embryos were allowed to develop to the specific stages, then dissected, fixed and processed for immunohistochemistry or in situ hybridization. For bromodeoxyuridine (BrdU) labeling, 5 μg/μl BrdU was injected into the neural tubes 1 or 4 hours prior fixation.

Immunohistochemistry

Embryos were fixed 2-4 hours at 4°C in 4% paraformaldehyde in PB, rinsed, sunk in 30% sucrose solution, embedded in OCT and sectioned in a Leica cryostat (CM 1900). Alternatively, embryos were section in a Leica vibratome (VT 1000S). Immunostaining was performed following standard procedures.

For BrdU detection, sections were incubated in 2N HCl for 30 minutes followed by 0.1 M $Na_2B_4O_7$ (pH 8.5) rinses further PBT rinses and anti-BrdU incubation.

Antibodies against the following proteins were used; green fluorescence protein (GFP) (Molecular Probes), anti-myc (9E10, Santa Cruz), a unique βIII-Tubulin (Tuj-1) (Medpass), phospho-Histone 3 (p-H3) (Upstate Biochemicals), NeuN (Chemicon), caspase 3 (BD), Bcl2 (Santa Cruz). Monoclonal antibodies to BrdU (G3G4), Pax7, Mnr2 (81.5C10), Nkx2.2 (74.5A5) were all obtained from the Developmental Studies Hybridoma Bank, developed under the auspices of the NICHD and maintained by The University of Iowa, Department of Biological Sciences, Iowa City, IA 52242.

Alexa488- and Alexa555-conjugated anti-mouse or anti-rabbit antibodies (Molecular Probes) were used. After single or double staining, sections were mounted, analyzed and photographed using a Leica Confocal microscope.

Cell counting was carried out on 10-40 different sections of at least four different embryos after each experimental condition (n>4).

In situ hybridization

Embryos were fixed overnight at 4°C in 4% paraformaldehyde in PB, rinsed and processed for whole-mount RNA in situ hybridization following standard procedures using probes for chick *N-myc* and *cyclinD1* (from the chicken EST project, UK-HGMP RC).

Hybridization was revealed by alkaline phosphatase-coupled anti-digoxigenin Fab fragments (Boehringer Mannheim). Hybridized embryos were postfixed in 4% paraformaldehyde, rinsed in PBT and vibratome sectioned.

TUNEL assay

Detection and quantification of apoptosis (programmed cell death) was performed using the 'In Situ Cell Death Detection Kit-POD conjugated' from Roche, following manufacturer's instructions.

Western blot

HH stage 11-12 embryos were electroporated with $Gli3A^{HIGH}$, neural tubes dissected at 12 and 24 hours post electroporation were collected in PBS and directly lysed in 1×SDS loading buffer [10% glycerol, 2% SDS, 100 mM DTT and 60 mM Tris-HCl (pH 6.8)] and the DNA disrupted by sonication. Samples were normalized by total protein content, separated by SDS-PAGE gel electrophoresis and transferred to nitrocellulose membranes, blocked with 8% non fat dry milk in TTBS [137 mM NaCl; 0.05 Tween 20 and 20 mM Tris-HCl (pH 7.4)], and probed with anti-Bcl2 antibody (Santa Cruz). The blots were developed using anti-rabbit coupled peroxidase plus the ECL system (Amersham). Quantifications were performed using a Biorad Chemiluminiscence Analyser (VERSADOC 5000).

Fluorescence associated cell sorting (FACS)

EGFP-containing plasmid DNA was injected into the lumen of HH stage 11-12 neural tube, embryos were electroporated as described above, and neural tubes dissected out 12-24 hours later. Single cell suspension was obtained by 10-15 minutes incubation in Trypsin-EDTA (Sigma). At least three independent experiments were analyzed by FACS for each experimental condition.

Hoescht and GFP fluorescence were determined by flow cytometry using a MoFlo flow cytometer (DakoCytomation, Fort Collins, CO). Excitation of the sample was carried out using a Coherent Enterprise II argon-ion laser. Excitation with the blue line of the laser (488 nm) permits the acquisition of forward-scatter (FS), side-scatter (SS) and green (530 nm) fluorescence from GFP. UV emission (40 mW) was used to excite Hoescht blue fluorescence (450 nm). Doublets were discriminated using an integral/peak dotplot of Hoechst fluorescence. Optical alignment was based on optimized signal from 10 μm fluorescent beads (Flowcheck, Coulter Corporation, Miami, FL). DNA analysis (Ploidy analysis) on single fluorescence histograms was done using Multicycle software (Phoenix Flow Systems, San Diego, CA).

RESULTS

Shh/Ptc1 signaling is required for cell cycle progression and cell survival

Shh signaling has been implicated in controlling the survival and proliferation of cells in a number of different tissues including progenitors of the neural tube. To confirm these observations and to

establish a system for further analysis, we examined the effect of blocking Shh signaling in individual neuroepithelial cells in the chick neural tube. To accomplish this we introduced, via in ovo electroporation, a dominant active form of the Hh receptor Patched1 (termed Ptc1$^{\Delta loop2}$). This version of Ptc1 lacks most of the second large extracellular loop and has lost the capacity to bind Shh but retains the ability to inhibit Smoothened or a downstream Smoothened effector, and inhibits Shh signaling in a cell-autonomous manner (Briscoe et al., 2001). To allow informative comparisons between embryos and constructs, we standardized the conditions used in all experiments: HH11-12 embryos were electroporated with each construct and following incubation and processing, analysis was restricted to the forelimb and the anterior thoracic regions.

In embryos expressing Ptc1$^{\Delta loop2}$ the transfected side of the neural tubes was noticeably reduced at 24 hours post-electroporation (PE) (Fig. 1A-D), suggesting that blocking Shh signaling inhibits cell proliferation and/or increases cell death. We first analyzed proliferation in transfected embryos. The number of mitotic cells, assessed by the marker phospho-Histone3 (pH3), was reduced by ~33% in the Ptc1$^{\Delta loop2}$ transfected side of the neural tube compared with the non-transfected control side of the neural tube [ratio of pH3+ cells EP versus non-EP neural tube: pCIG 24h-PE 1.00±0.09 pH3+ cells (n=4); Ptc1$^{\Delta loop2}$ 24h-PE 0.68±0.1 pH3+ cells (n=3) (P=0.0012)] (Fig. 1A,M). Moreover, pulse labeling electroporated embryos with bromodeoxyuridine (BrdU) indicated that entry of neuroepithelial cells into S-phase of the cell cycle, was also decreased (~46% reduction) in cells transfected with Ptc1$^{\Delta loop2}$ compared with control cells transfected with the empty vector pCIG [24h-PE 29.77±5.75% of GFP+ cells in pCIG embryos incorporate BrdU ventrally and 27.14±1.24% dorsally (n=2); 12.87±3.49% of Ptc1$^{\Delta loop2}$ transfected cells incorporate BrdU ventrally (P=0.0024) and 17.14±6.57% dorsally (n=2)

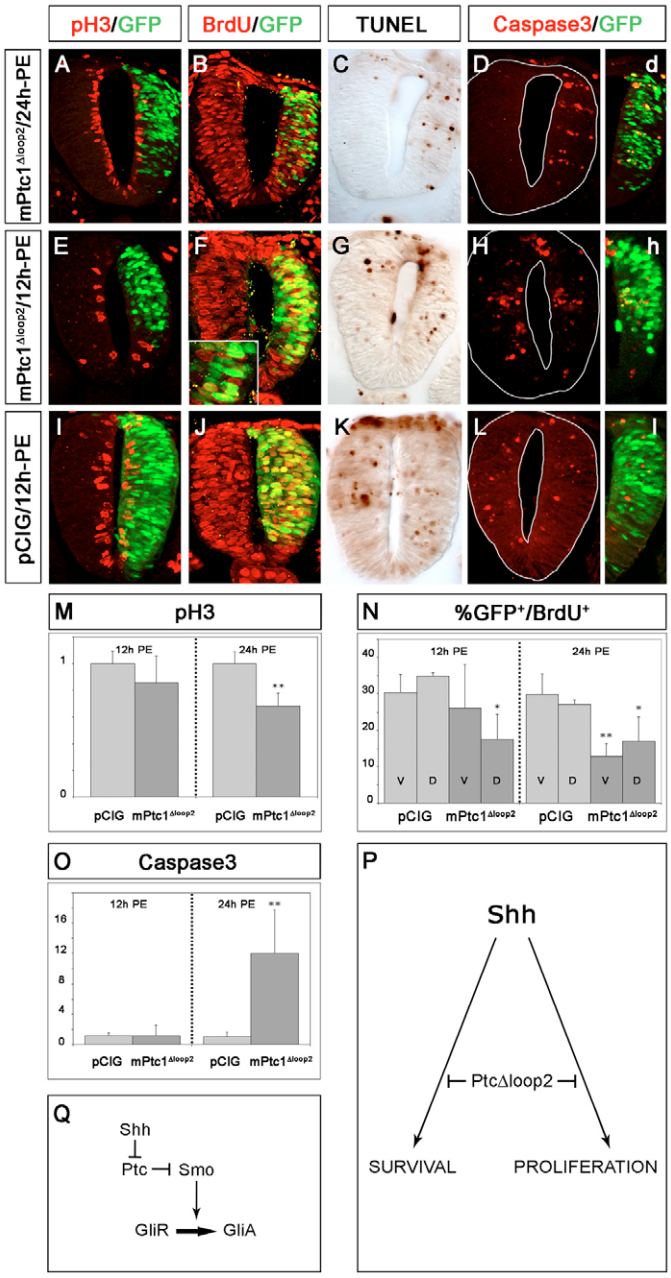

Fig. 1. Transfection of Ptc1$^{\Delta loop2}$ inhibits neural cell proliferation and survival. HH11/12 stage chick embryos were electroporated in ovo with a bi-cistronic vector containing Ptc1$^{\Delta loop2}$ and GFP, or with the empty vector (pCIG-GFP) as control, and assayed 12 and 24 hours post-electroporation (PE) for the indicated markers. Transfected side of the neural tube is to the right side of the figures. (**A-D**) 24 hours PE of Ptc1$^{\Delta loop2}$ caused reduction of pH3-immunostaining on the transfected side, compared with the control contralateral side (A). BrdU incorporation is reduced in GFP-positive cells. Electroporated GFP-positive cells that have entered S phase of the cell cycle are yellow (B). TUNEL staining (brown) is increased in Ptc1$^{\Delta loop2}$ (C) and activated caspase 3-immunostaining is also increased (D). (**E-H**) Ptc1$^{\Delta loop2}$ neural tubes 12 hours PE show a reduction in pH3 immunostaining (E). BrdU incorporation is reduced in GFP-positive cells (F). TUNEL (G) and caspase 3 immunostaining (H) are not increased on the electroporated side 12 hours PE. (**I-L**) Control embryos transfected with the empty vector (pCIG) identified by GFP (green) and analyzed 12 hours PE, show an equal number of pH3-immunostaining cells on the electroporated side compared with non-electroporated side (I), GFP-positive cells can incorporate BrdU, as indicated by the elevated proportion of double-labeled yellow cells (J). TUNEL staining (K) and activated caspase 3 immunostaining (L) are the same on transfected side and control contralateral side. (**M**) Quantitative analysis of pH3-immunostained cells in electroporated and non-electroporated sides of the neural tube. 12 hours PE there was no significant changes in pH3 immunostaining; however, 24 hours PE, the number of pH3 cells in Ptc1$^{\Delta loop2}$ EP embryos was significantly reduced on the transfected side of the neural tube. Error bars indicate s.d. (**N**) Quantitative analysis of Ptc1$^{\Delta loop2}$-GFP/BrdU double labeled cells in ventral and dorsal neural tubes, after a 4-hour BrdU pulse indicated a decrease of ~15% in ventral regions and ~50% in dorsal regions of the number of cells incorporating BrdU by 12 hours PE, and a ~60% decrease in ventral regions and ~40% decrease in dorsal regions by 24 hours PE. Error bars indicate s.d. (**O**) Quantitative analysis of activated caspase 3-positive cells in electroporated compared with non-electroporated side. 12 hours PE there was no increase in caspase 3 immunostaining, while 24 hours PE there was a ~12 fold increase in caspase 3 immunostaining in neural tubes transfected with Ptc1$^{\Delta loop2}$. Error bars indicate s.d. (M-O) *P<0.05; **P<0.005; ***P<0.0001 control versus treated. (**P**) Summary of the effect of Ptc1$^{\Delta loop2}$ on neuroepithelial cells. (**Q**) Schematic representation of the Shh pathway.

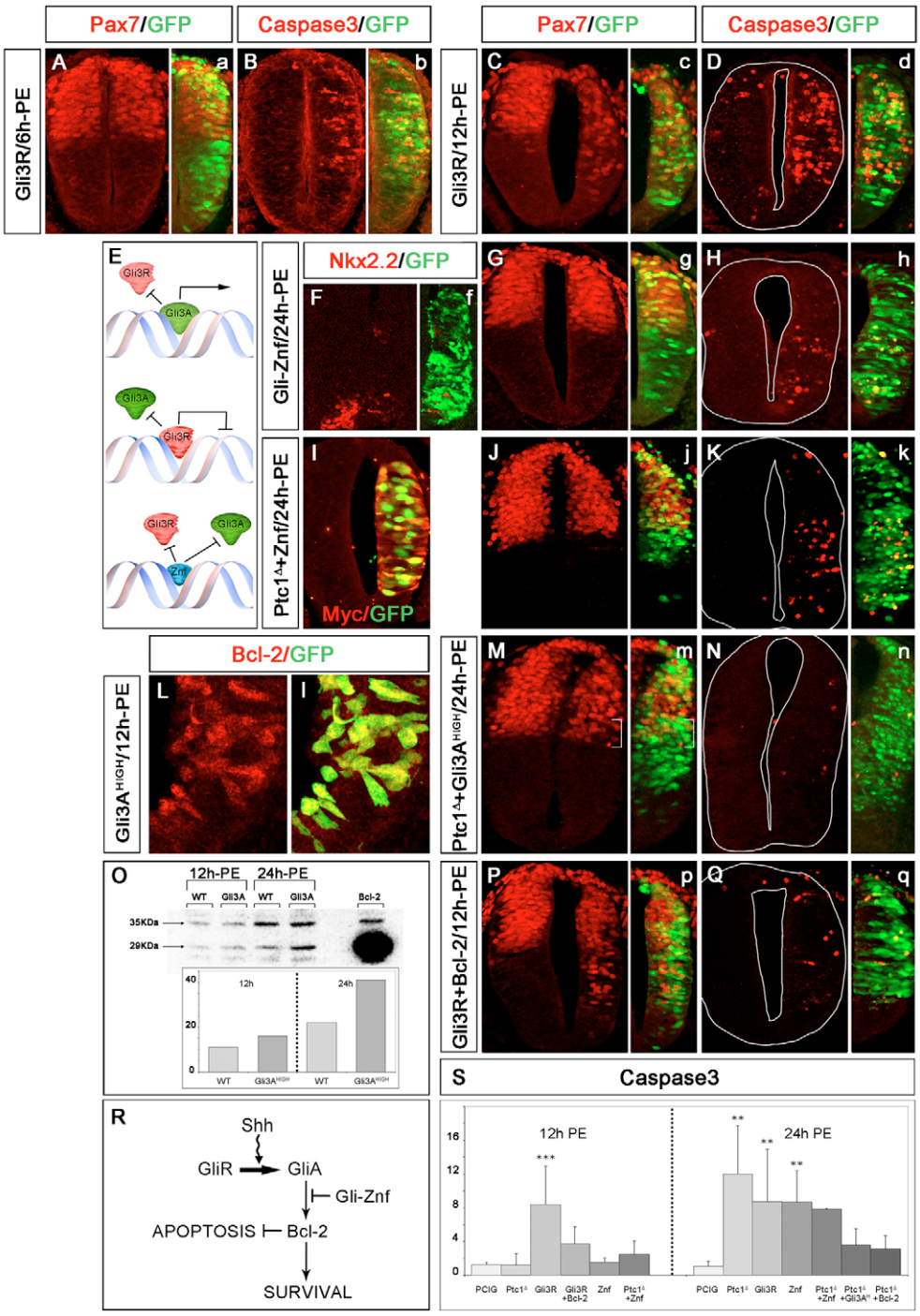

Fig. 2. See next page for legend.

(P=0.0057)] (Fig. 1B,N). The combined visualization of GFP, to assess cell transfection, with anti-BrdU immunostaining indicated that the blockade of cell cycle progression was cell autonomous (Fig. 1B,F), while adjacent untransfected cells continued to incorporate BrdU (Fig. 1F, inset). We next analyzed apoptosis in transfected embryos. Comparing the side of the neural tube transfected with Ptc1$^{\Delta loop2}$ with the control non-transfected side indicated a significant increase in TUNEL staining (Fig. 1C) and immunoreactivity for the apoptotic marker caspase 3 [24h-PE pCIG embryos contain 1.02±0.64 caspase3+ cells/section (n=4), Ptc1$^{\Delta loop2}$ embryos contain 11.99±5.74 caspase 3^{+} cells/section (n=4) (P=0.0002)] (Fig. 1D,O). Thus, by 24 hours PE, blockade of Shh signaling in neuroepithelial cells inhibits both cell cycle progression and cell survival.

We next examined the phenotype of embryos 12 hours PE. A noticeable decrease in the size of the transfected side of the neural tube was also apparent in these embryos (Fig. 1E-H). In contrast to embryos at 24 hours PE, however, at 12 hours PE there was no increase in the apoptosis marker caspase 3 (Fig. 1H,L,O) or in TUNEL staining (Fig. 1G,K). However,

Fig. 2. Gli transcriptional activation is required for neural cell survival. HH11/12 stage chick embryos were electroporated in ovo with a bi-cistronic vector containing the indicated plasmids and assayed, at the indicated times, for activated caspase 3 immunostaining as a marker for apoptotic cell death. (**A-D**) Repressor forms of Gli (Gli3R) cause high levels of apoptosis prior to inducing cell fate changes. (**A**,**B**) At 6 hours PE, Pax7 expression (red) is normal; however, caspase 3 immunostaining is highly activated on the electroporated side (B). (**C**,**D**) At 12 hours PE, Pax7 is ectopically expressed in ventral regions of the electroporated neural tube (C), together with an increased level of caspase 3 immunostaining (D). (**E**) Representation of Gli-variants transfected into the neural tube. Gli3A^{HIGH} acts as a constitutive transcriptional activator. Gli3R acts as a constitutive transcriptional repressor form. Gli-ZnF inhibits both Gli repression and activation. (**F-H**) Expression of Gli-ZnF results in lack of activation of Nkx2.2 (F) and normal expression of Pax7 (G); however, Gli-ZnF causes increased caspase 3 immunostaining (H). (**I-K**) Blocking Gli-transcriptional activity does not rescue Ptc1$^{\Delta loop2}$-induced apoptosis. Embryos were co-electroporated with Gli-ZnF/Myc and Ptc1$^{\Delta loop2}$/GFP. (I) Immunostaining with anti-Myc (red) and GFP fluorescence (green) revealed a high proportion of cells co-transfected with both plasmids. (J,K) At 24 hours PE of Gli-ZnF+ Ptc1$^{\Delta loop2}$, expression of Pax7 was normal (J); however, caspase 3 immunostaining was increased (K). (**L**) Gli-activator proteins induce expression of the survival gene Bcl2. At 12 hours PE of Gli3A^{HIGH}, there is increased Bcl2 immunostaining (red) in electroporated cells (green). (**M**,**N**) Gli-activator proteins rescue Ptc1$^{\Delta loop2}$-induced cell fate changes and apoptosis. (M) Embryos electroporated with Ptc1$^{\Delta loop2}$+Gli3A^{HIGH} demonstrate cell-autonomous downregulation of dorsal Pax7. Moreover, there is no increase in the level of activated caspase 3 (N). (**O**) Neural tubes electroporated with Gli3A^{HIGH} were collected 12 and 24 hours PE for western blot analysis. Low levels of Bcl2 protein (29 kDa) were detected in control sides (WT). Expression of Bcl2 was moderately increased by 12 hours PE (GliA). A twofold increase in protein levels was detected 24 hours PE (GliA). Uniformity of protein loading was confirmed by uniform levels of a 35 kDa marker band. Chemiluminiscence was quantified using a Biorad Analyzer. (**P,Q**) Transfection of human BCL2 rescues Gli3R induced apoptosis but not cell fate changes. Embryos co-transfected with human BCL2+Gli3R had ectopic ventral expression of Pax7 (P); however, the levels of activated caspase 3 were normal in human BCL2+Gli3R co-electroporated neural tubes (Q). (**R**) Summary of Shh/Gli activities on neuroepithelial cell survival. (**S**) Quantitative analysis of caspase 3-positive cells in electroporated versus non-electroporated sides of the neural tube. 12 hours PE there was a significant increase in apoptosis induced by Gli3R this was prevented by co-electroporation of BCL2. Ptc1$^{\Delta loop2}$ also significantly increase apoptosis at 12 hours PE which was prevented by the co-electroporation of either Gli-ZnF, Gli3A^{HIGH} or human BCL2. Error bars indicate s.d. *P<0.05; **P<0.005; ***P<0.0001 control versus treated.

proliferation was affected with the number of cells in mitosis fewer on the transfected side of the neural tube, than on the control non-transfected side [ratio of pH3+ cells EP versus non-EP neural tube: pCIG 12h-PE 1.00±0.09 pH3+ cells (n=4); Ptc1$^{\Delta loop2}$ 12h-PE 0.86±0.2 pH3+ cells (n=4)] (Fig. 1E,I,M). Quantitation indicated a decrease of ~15% in ventral regions and ~50% in dorsal regions in the number of transfected cells incorporating BrdU [12h-PE 30.35±5.03% of GFP+ cells in pCIG embryos incorporate BrdU ventrally and 34.91±1.05% dorsally (n=2); by contrast, 26.17±11.95% of Ptc1$^{\Delta loop2}$ transfected cells incorporate BrdU ventrally (P=0.0024) and 17.51±6.89% dorsally (n=2) (P=0.017)] (Fig. 1F,J,N). These data indicate that blockade of Shh signaling results in a decreased rate of neuroepithelial cell cycle progression within 12 hours PE and this occurs prior to onset of apoptotic cell death.

These data prompted us to ask whether Shh signaling is required to maintain neural precursor cell proliferation at later stages of neural development. Embryos electroporated at stage HH14 and analyzed 48 hours PE also showed a reduction in the size of the electroporated neural tube and a significant cell-autonomous reduction in the number of GFP/BrdU double-labeled cells (see Fig. S1A-D in the supplementary material). Similar results were obtained with embryos electroporated at stage HH18 and analyzed by 48 hours PE (see Fig. S1E-H in the supplementary material). Increased levels of apoptosis were also apparent on the transfected side of these embryos (see Fig. S1I,J in the supplementary material).

Together, the data indicate that active Shh signaling is required for cell cycle progression and cell survival and suggest that Ptc1 acts directly on cells to regulate these properties. To test for a role of the canonical Shh/Gli pathway on these effects, we next analyze the effects of introducing different version of Gli proteins.

Gli activator protein promotes neural cell survival

Although the evidence suggests that all patterning activities of Shh are Gli dependent (Jeong and McMahon, 2005; Lei et al., 2004; Bai et al., 2004; Meyer and Roelink, 2003; Persson et al., 2002), it is unclear whether Gli dependent transcription is required for the Shh mediated survival of cells. Thibert et al. (Thibert et al., 2003) have provided evidence that, in the absence of the ligand Shh, the receptor Ptc1 acts as a transmembrane death receptor able to activate the caspase cascade independently of Smoothened signaling and Gli-mediated transcription. However, in the developing limb, Gli-dependent transcription has been suggested to mediate cell survival/apoptosis (Bastida et al., 2004).

To test for an involvement of Gli-mediated transcription in the apoptosis/survival of neural progenitors, we first examined whether introducing a dominant inhibitor of Gli dependent transcription affected cell survival. We transfected a deleted form of Gli3 (Gli3R) that contains the N-terminal repressor and the zinc-finger, DNA-binding domains that are equivalent to the proposed proteolytically processed form of Gli3 (Wang et al., 2000). In vitro, Gli3R blocks all Shh/Gli-mediated transcriptional activation acting as a dominant inhibitory Gli protein, and in vivo Gli3R blocks the Shh-mediated ventralization of the neural tube (Meyer and Roelink, 2003; Persson et al., 2002). Stage HH11/12 chick embryos electroporated with Gli3R and assayed 12 hours PE showed the expected ectopic ventral activation of Pax7 (Fig. 2A,C). Moreover, transfection of Gli3R caused a marked and very rapid induction of cell death (by 6 hours PE) (Fig. 2B) that reached a maximum 12 hours PE [ratio of apoptotic cells at 12h-PE, EP versus non-EP sides, in pCIG embryos is 1.24±0.34 cells (n=4), the ratio in Gli3R embryos is 8.35±4.57 (n=5) (P<0.0001)] (Fig. 2D,S). These data indicate that, similar to the ectopic expression Ptc1$^{\Delta loop2}$, blocking Gli dependent transcription induces neuroepithelial cell apoptosis. This increase in apoptosis was also apparent at 6 hours PE and occurred prior to detectable changes in the regulation of progenitor expressed transcription factors that respond to Shh signaling (Fig. 2A,B). Together, these data raise the possibility that the apoptosis induced by Ptc1$^{\Delta loop2}$ is a consequence of increased Gli repressor activity.

To address this, we took advantage of a deleted form of Gli3 protein that contains only the DNA-binding zinc-finger-domain (Gli-ZnF, Fig. 2E). In vivo, Gli-ZnF is unable to activate transcription of

class II homeodomain (HD) proteins such as Nkx2.2 (Fig. 2F) or to de-repress transcription of class I HD proteins such as Pax7 (Fig. 2G); in vitro it blocks both positive and negative Gli activity (data not shown). This indicates that Gli-ZnF lacks both Gli-mediated transcriptional activation and repression activities. In Gli-ZnF-transfected embryos analyzed 24 hours PE, neural tubes contained increased caspase 3 immunostaining [ratio of apoptotic cells, EP versus non-EP sides, 8.66±3.76 (n=4) compared with 1.02±1.55 (n=6) (P=0.0002)] (Fig. 2H,S). This suggests the possibility that the increased apoptosis in Ptc1$^{\Delta loop2}$ transfected embryos might be due to a reduction in positive Gli transcriptional activity.

We next asked whether Ptc- and Gli-mediated apoptosis were two independent events. To test whether Ptc1$^{\Delta loop2}$ mediated apoptosis of neuroepithelial cells was dependent on Gli activity, we analyzed embryos that were co-electroporated with Ptc1$^{\Delta loop2}$ and the Gli-ZnF constructs. Co-expression of both constructs was monitored by immunostaining with the anti-Myc antibody as a reporter of the Gli-ZnF expression and GFP as a reporter of Ptc1 expression (Fig. 2I). Lack of Gli transcriptional activity inhibited the Ptc1$^{\Delta loop2}$-induced ventral expansion of Pax7 (Fig. 2J), suggesting that it was dependent on Gli-repressor activity (Briscoe et al., 2001). However, the level and kinetics of apoptosis assessed by caspase 3 immunostaining was similar in co-electroporated embryos (Fig. 2K,S) to that seen in embryos electroporated independently with Ptc1$^{\Delta loop2}$ and with Gli-ZnF [At 12 hours PE in Gli-ZnF the ratio (EP versus non-EP side) of apoptotic cells is 1.58±0.45 cells (n=4); in Ptc1$^{\Delta loop2}$+ZnF the ratio is 2.50±1.55 (n=6). At 24 hours PE, in Gli-ZnF the ratio is 8.66±3.76 (n=4) (P=0.0002); and in Ptc1$^{\Delta loop2}$+Gli-ZnF the ratio is 7.86±0.08 (n=4).] (Fig. 1D, Fig. 2H,S). The absence of a synergistic effect in co-electroporated embryos is consistent with the idea that the induction of apoptosis in Ptc1$^{\Delta loop2}$ transfected cells is due to a decrease in Gli transcriptional activity. Moreover, the fact that the Gli-ZnF construct rescues changes in cell fate but not the increased apoptosis, suggests that Shh signaling regulates the survival of neural progenitors independent of patterning.

To test whether Ptc1$^{\Delta loop2}$-mediated apoptosis was dependent on Gli transcriptional repression, we examined whether providing Gli transcriptional activity was sufficient to promote the survival of cells expressing Ptc1$^{\Delta loop2}$. To achieve this, we took advantage of a dominant active form of Gli3 from which the entire N-terminal/repressor domain was deleted (hGli3$^{\Delta N2}$) (Stamataki et al., 2005). This construct provides strong transcriptional activation in vitro and in vivo (Gli3A^{HIGH}) (Stamataki et al., 2005). HH stage 11-12 chick embryos co-electroporated with Ptc1$^{\Delta loop2}$ and Gli3A^{HIGH}, assayed 24 hours PE displayed the expected cell autonomous downregulation of the dorsal marker Pax7 together with the suppression of the ventral expansion of Pax7 induced by Ptc1$^{\Delta loop2}$ (Fig. 2M). Moreover, expression of Gli3A^{HIGH} was sufficient to inhibit Ptc1$^{\Delta loop2}$-induced apoptosis. The transfected side of the neural tube of co-electroporated embryos no longer displayed the shortening characteristic of Ptc1$^{\Delta loop2}$ transfectants and assays for caspase 3 immunostaining (Fig. 2N) and TUNEL (not shown) indicated that co-electroporated embryos had wild-type levels of apoptosis [the ratio of apoptotic cells in the neural tube co-electroporated with Ptc1$^{\Delta loop2}$ + Gli3A^{HIGH} is 3.61±1.88 (n=4) compared with 11.99±5.74 (n=4) in Ptc1$^{\Delta loop2}$-alone embryos] (Fig. 2S). Together, these data suggest that Gli dependent transcription mediates Ptc1-induced apoptosis of neural tube progenitors, and indicate that Gli3 is epistatic to Ptc1$^{\Delta loop2}$ for both activities.

In keratinocytes, the anti-apoptotic factor Bcl2 has been shown to be induced by Gli-dependent transcription (Bigelow et al., 2004; Regl et al., 2004). We therefore asked whether Bcl2 is induced by

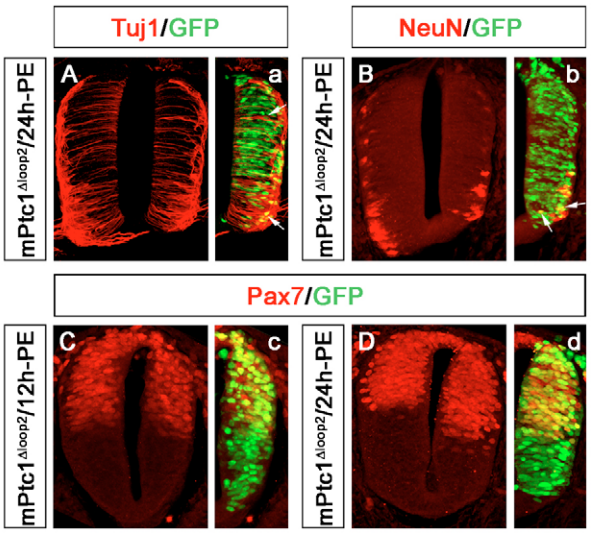

Fig. 3. Loss of Shh/Ptc1-signaling does not inhibit or promote neuron differentiation. (**A**,**B**) HH stage 11/12 chick embryos electroporated with Ptc1$^{\Delta loop2}$, were analyzed 24 hours later for GFP expression (green) and molecular markers for neural differentiation (red). (A) Immunostaining with the Tuj1 antibody (red) revealed the presence of Ptc1$^{\Delta loop2}$-transfected cells expressing Tuj1 (arrows indicate co-expressing cells). (B) Immunostaining with NeuN revealed the presence of transfected cells expressing NeuN (yellow cells). (**C**,**D**) Loss of Shh/Ptc1 signaling causes cell fate changes 24 hours PE. (C) At 12 hours PE of Ptc1$^{\Delta loop2}$, Pax7 expression is comparable on both sides of the neural tube. (D) At 24 hours PE, Pax7 expression is ventrally induced on the transfected side of the neural tube.

Gli-transcriptional activation in neuroepithelial cells. Indeed, electroporation of Gli3A^{HIGH} was sufficient to induce Bcl2 expression cell autonomously, as detected by immunohistochemistry (Fig. 2L). Furthermore, western blot analysis revealed low levels of Bcl2 expression on control side and a two-fold increase in Bcl2 protein levels in neural tubes 24 hours after electroporation of Gli3A^{HIGH} (Fig. 2O). Thus, Bcl2 seems to be a conserved Gli-transcriptional survival target, functioning also in neuroepithelial cells. We next reasoned that as Bcl2 was a target of Gli-transactivation, overexpression of Bcl2 may rescue Ptc1$^{\Delta loop2}$ and Gli3R induced apoptosis. Consistent with this idea, forced expression of human BCL2, together with Ptc1$^{\Delta loop2}$ (Fig. 2S) or with Gli3R (Fig. 2P,Q,S) reduced the levels of apoptosis in transfected neural tubes [the ratio of apoptotic cells in the neural tube of embryos co-electroporated with Ptc1$^{\Delta loop2}$ +human BCL2 is 3.14±1.60 cells (n=4) and in Gli3R+BCL2 is 3.72±2.04 (n=4)]. Thus, these results indicate that Bcl2 overexpression is sufficient for the survival of neuroepithelial cells and suggests that basal levels of Gli-mediated induction of Bcl2 may be required for survival of neuroepithelial cells.

Gli activity regulates progression of progenitor cell cycle

We next turned our attention to the regulation of neural progenitor proliferation by Shh signaling. During neural tube development, as neuroepithelial cells differentiate they exit the cell cycle and become post-mitotic. As blockade of Shh/Ptc signaling decreased cell cycle progression, one possibility was that in the absence of Shh signaling there was increased neuronal differentiation of progenitors and a concomitant decrease in the number of proliferating cells. To test this,

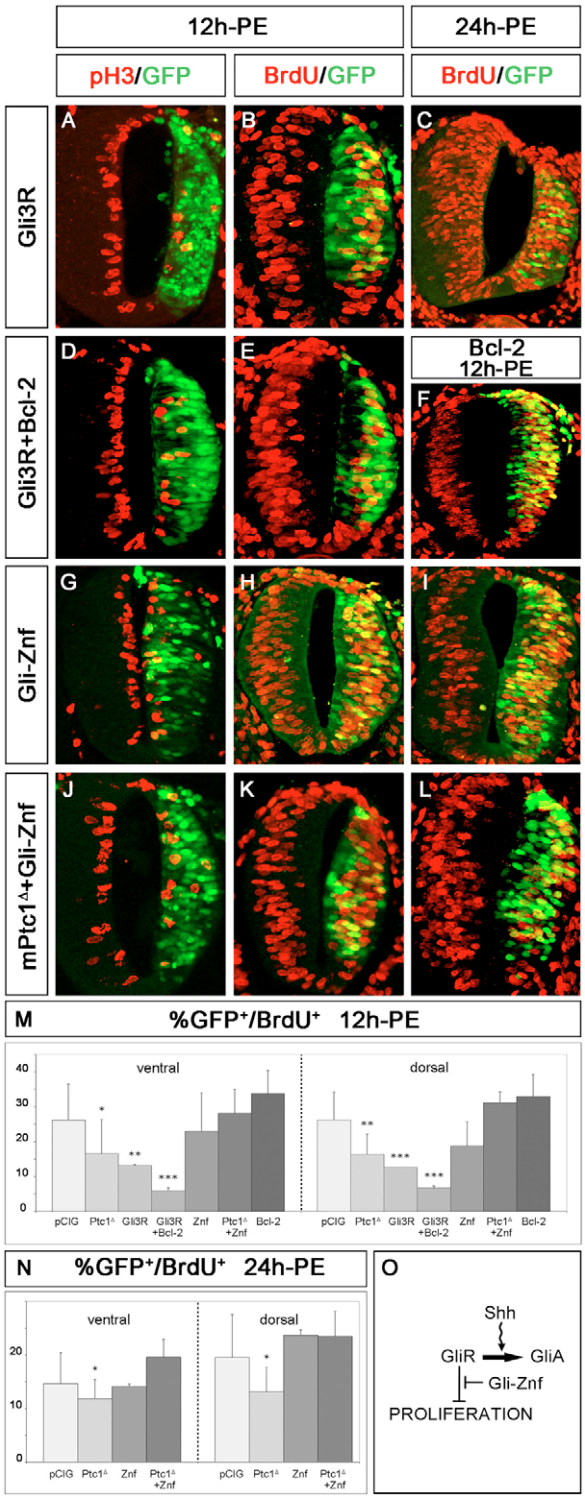

Fig. 4. Repressor forms of Gli (Gli3R) cause cell cycle arrest. HH stage 11/12 embryos electroporated with the indicated plasmids, were analyzed for cell proliferation by immunostaining with the mitosis marker pH3 and by incorporation of BrdU for 1 hour, in ovo. (**A-C**) Repressor forms of Gli (Gli3R) cause cell cycle arrest. (A) At 12 hours PE, the number of mitotic cells is reduced in the electroporated side. (B) Few electroporated cells can enter the S phase of the cell cycle, as revealed by the number of GFP-expressing cells (green) that can incorporate BrdU (red) and thus are double labeled (yellow). (C) At 24 hours PE, the electroporated side of the neural tube is reduced and there is a clear reduction in the number of GFP/BrdU double-labeled cells. (**D,E**) Embryos co-transfected with Gli3R+human BCL2 and analyzed 12 hours PE display reduced pH3 staining (D) and reduced BrdU incorporation (E). (**F**) Embryos transfected with Bcl2 have normal rates of proliferation. (**G-I**) Embryos transfected with Gli-ZnF have a normal sized neural tube, and a normal rate of proliferation. (G) At 12 hours PE, pH3 immunostaining is comparable on both sides of the neural tube. A high proportion of Gli-ZnF electroporated cells can incorporate BrdU, as assessed by double labeling, either at 12 hours PE (H) or 24 hours PE (I). (**J-L**) Blocking Gli-transcriptional activity rescues $Ptc1^{\Delta loop2}$-induced cell cycle arrest and the size reduction in the neural tube. At 12 hours PE of $Ptc1^{\Delta loop2}$+Gli-ZnF, pH3-immunostained cells are comparable on both sides of the neural tube (J). A high proportion of $Ptc1^{\Delta loop2}$+Gli-ZnF electroporated cells can incorporate BrdU, as assessed by double labeling, either at 12 hours PE (K) or at 24 hours PE (L). (**M**,**N**) Quantitative analysis of GFP-expressing cells (green) that have incorporated BrdU (red), after a 1 hour BrdU pulse. Analysis was carried out by separating dorsal and ventral halves of the neural tube. At 24 hours PE, the number of cells incorporating BrdU increased ~15% in ventral regions and ~50% in dorsal regions in $Gli3A^{HIGH}$ transfected embryos. (**O**) Summary of Shh/Gli activities on proliferation of neuroepithelial cells. **P*<0.05; ***P*<0.005; ****P*<0.0001 control versus treated.

we combined the visualization of GFP with antibody staining for two pan-neural markers Tuj1 and NeuN. In embryos transfected with $Ptc1^{\Delta loop2}$, there was no increase in the number of post-mitotic neurons at 24 hours PE, thus the decrease in progenitor proliferation could not be accounted for by precocious differentiation of neuroepithelial cells. Moreover, by 24 hours PE there were fewer differentiated neurons on the $Ptc1^{\Delta loop2}$ transfected side of the embryo compared with the control side (Fig. 3A,B). This most likely reflects the general reduction in tissue size caused by the $Ptc1^{\Delta loop2}$ expression: the lack of Shh signaling did not appear to inhibit neural differentiation in a cell-autonomous manner, as many GFP-positive transfected cells were also NeuN and Tuj1 positive (Fig. 3A,B). Moreover, the decrease in proliferation was apparent prior to changes in the expression of transcription factors regulated by Shh signaling, that control progenitor cell identity. For example, in embryos transfected with $Ptc1^{\Delta loop2}$, the changes in the expression of Pax7 were observed at 24 hours PE (Fig. 3D) but at 12 hours PE, a time point at which a decrease in progenitor proliferation was apparent, the expression of Pax7 was comparable with the non-transfected control side of the neural tube (Fig. 3C). Together, these data raise the possibility that Shh/Ptc signaling directly regulates cell cycle progression.

We next sought to determine whether Gli-mediated transcription, downstream of Shh/Ptc signaling, regulates cell cycle progression. The observation that, Ptc1 interacts directly with cyclin B1 (in the absence of the ligand, Shh), preventing nuclear translocation and regulating cell cycle progression in 293T cells (Barnes et al., 2001) left open the possibility that Ptc1 inhibits the cell cycle independent of Gli proteins. We first transfected the dominant inhibitory Gli protein, Gli3R, into stage HH11/12 chick embryos. Assays at 12 hours PE showed a reduction in the total number of mitotic cells (Fig. 4A) and a reduction in the number of transfected cells that can incorporate BrdU to ~50% [Gli3R expression reduced the proportion of transfected cells incorporating BrdU to 13.13±0.36% (n=4) (P=0.001) in the ventral neural tube and to 12.68±0.01% (n=4) (P<0.0001) dorsally compared with 26.25±10.19% ventrally and 26.18±8.02% dorsally in pCIG embryos] (Fig. 4B,M). Furthermore,

embryos analyzed 24 hours PE exhibited a dramatic reduction in the number of proliferating cells and size of the neural tube (Fig. 4C; data not shown). The severity of this phenotype most probably reflects the combined consequence of lack of proliferation together with enhanced cell death seen in embryos expressing Gli3R (Fig. 2B,D). Therefore, in order to analyze whether Gli3R regulated cell cycle progression independently of apoptosis, we co-electroporated Gli3R and human BCL2. Co-transfection of both plasmids was monitored by immunostaining with anti-Bcl2 and GFP fluorescence as a reporter of Gli3R (not shown). Embryos transfected with Gli3R+human BCL2, analyzed 12 hours PE had a significantly decreased proliferation rate, as assessed by pH3 immunostaining (Fig. 4D) and by BrdU incorporation (Fig. 4E,M). We observed a ~75% reduction in BrdU incorporation in Gli3R+human BCL2 transfected cells when compared with control pCIG-transfected progenitors (Fig. 4M) [6.69±0.62% cells in Gli3R+human BCL2 embryos are double labelled for GFP and BrdU (n=7) (P<0.0001) in the ventral and 5.92±0.82% (n=7) (P<0.0001) in the dorsal neural tube]. The enhanced blockade of cell cycle progression compared with embryos transfected with Gli3R alone, is probably the result of the survival of additional Gli3R-expressing cells and the fact that these cells do not enter S phase (Fig. 4M).

In order to test whether cell cycle arrest is mediated through active Gli repression or through the lack of Gli-transactivation, we blocked all Gli transcriptional activities using Gli-ZnF (Fig. 2E-H). Embryos analyzed either 12 or 24 hours PE of Gli-ZnF, showed normal rates of proliferation as assessed by either pH3 immunostaining (Fig. 4G) or BrdU incorporation (Fig. 4H,I). Furthermore, both halves of the neural tube were the same size, reflecting the normal growth of these neural tubes. These data indicate that the observed Gli3R-dependent cell cycle arrest might be due to active Gli-repression.

We next asked whether Ptc1-mediated cell cycle arrest of neuroepithelial cells was also dependent on Gli activity. Stage HH 11/12 chick embryos were co-electroporated with Ptc1$^{\Delta loop2}$ and Gli-ZnF and assayed at 12 and 24 hours PE. Total number of mitotic cells, assessed by immunostaining to pH3 was restored in co-electroporated embryos at both time points (Fig. 4J, data not shown). Furthermore, lack of Gli repression restored BrdU incorporation in a cell-autonomous manner, both by 12 hours PE [28.16±6.86% of Ptc1$^{\Delta loop2}$ +Gli-ZnF transfected cells incorporate BrdU (n=4) in the ventral and 31.11±3.11% cells (n=4) in the dorsal neural tube] (Fig. 4K,M) and 24 hours PE [in Ptc1$^{\Delta loop2}$ +Gli-ZnF embryos 19.65±3.28% cells are double-labelled of GFP/BrdU (n=4) in the ventral and 23.52±4.65% in the dorsal neural tube (n=4)] (Fig. 4L,N), strongly suggesting that Ptc1$^{\Delta loop2}$-dependent cell cycle arrest is mediated through Gli-repression.

Inhibiting Shh/Gli signaling lengths the G1 phase of the cell cycle

We next tested how transfection of Gli3-R modulated cell cycle phase distribution. For this purpose, neuroepithelial cells electroporated in ovo with the control vector pCIG±human BCL2 (Fig. 5A), with GLi3R (Fig. 5B) or with Gli3R+human BCL2 (Fig. 5C) were analyzed by flow cytometry. This analysis indicated that in control conditions, 12 hours PE, 59% of cells were in the G1 phase of the cell cycle (1N DNA content), 23% in S phase (intermediate DNA content) and 18% in G2/M phase (2N DNA content) (Fig. 5D). Gli3R transfection caused a dramatic increase in apoptosis and generated a very abnormal cell cycle profile, with a sub-G1 population that probably corresponds to dead and dying cells (Fig. 5B). Therefore, we analyzed the cell cycle of neuroepithelial cells that were co-transfected with Gli3R+human BCL2. The restoration of the cell cycle profile in these cells confirmed the anti-apoptotic effect of Bcl2 (Fig. 5C) and in these conditions the proportion of transfected cells in G1 had increased to 71%, while only 15% of cells were in S phase and 14% cells were in G2/M phase (Fig. 5D). These data suggest that transfection of Gli3R prevents entry of neuroepithelial cells into the S phase of the cell cycle and results in cells accumulating in G1.

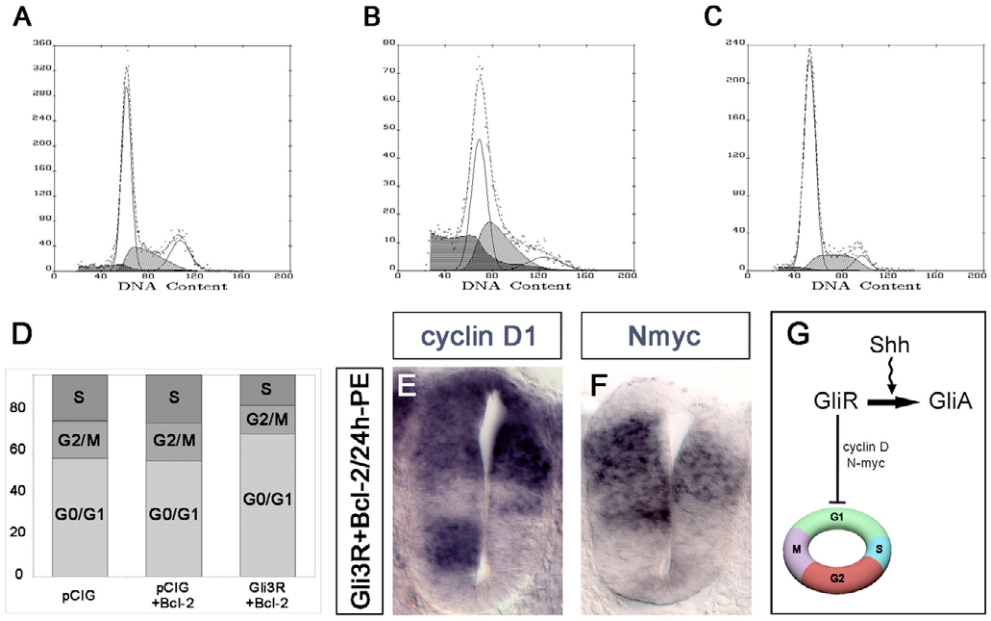

Fig. 5. Flow cytometry analysis of cell cycle phase distribution of transfected cells. HH stage 11/12 embryos were electroporated with pCIG, pCIG+human BCL2, Gli3R and Gli3R+human BCL2-containing vectors. At 12 hours PE, neural tubes were dissected out, GFP-expressing cells separated by flow cytometry and cell cycle phases analyzed by Hoescht staining. (**A-C**) Representative examples of cell cycle profile of cells expressing pCIG (A), Gli3R (B) and Gli3R+human BCL2 (C). The sub-G1 cell population observed in Gli3R-electroporated cells corresponds to dead and dying cells (B). (**D**) Cell cycle phase distribution of transfected cells. At 12 hours PE, in Gli3R transfected embryos there was a ~12% increase in the number of cells accumulating at G0/G1 phase of the cell cycle. (**E**,**F**) Gli3-R repressed transcription of genes involved on G1 transition. (E) In situ hybridization with a chick *cyclin D1* probe, 12 hours PE of Gli3R+human BCL2. The ventral domain of *cyclin D1* expression is lacking on the electroporated side of the neural tube. (F) In situ hybridization with a chick *N-myc* probe, 12 hours PE of Gli3R+human BCL2. *N-myc* expression is repressed on the electroporated side. (**G**) Summary of Shh/Gli activities on cell cycle progression of neuroepithelial cells.

Consistent with a G1 block in cell cycle progression, the expression of cyclin D1, a cyclin characteristic of G1 progression, was repressed, at least in ventral regions of Gli3R-transfected neural tubes (Oliver et al., 2003; Kenney and Rowitch, 2002) (Fig. 5E). Noteworthy, however, was the continued cyclin D1 expression in dorsal neural progenitors, suggesting that the cell cycle block initiated by Gli3R may involve the regulation of genes in addition to cyclin D1. Expression of N-myc, a Shh-target gene promoting proliferation of cerebellar granule precursors (Kenney et al., 2003) was also repressed in Gli3R+human BCL2 electroporated neural tubes (Fig. 5F). Together these data suggest that Gli-mediated repression of genes required for completion of the G1 phase of the cell cycle, cause cell cycle arrest of neuroepithelial cells.

Activator Gli-proteins induce overproliferation

It has previously been shown that dorsal activation of the Shh-pathway by either ectopic expression of the ligand (Rowitch et al., 1999) or by the introduction of a dominant-negative form of PKA (Epstein et al., 1996) caused a prominent overgrowth of the dorsal neural tube. HH11-12 embryos electroporated with this same dnPKA construct show the expected changes in patterning 24 and 48 hours PE (see Fig. S2A-C in the supplementary material), together with increased proliferation on neural tubes (see Fig. S2D-I in the supplementary material).

Therefore, we asked whether Gli-transcriptional activity is sufficient to increase the proliferation of neuroepithelial cells. To test this, we transfected neural tube cells with Gli3A^{HIGH} and analyzed 24 hours PE. Gli3A^{HIGH}-transfected cells showed the expected cell-autonomous downregulation of dorsal markers such as Pax7 (Fig. 6A) and activation of ventral markers such as Mnr2 (Fig. 6B). Moreover, transfection of Gli3A^{HIGH} caused overgrowth of the electroporated side of the neural tube (Fig. 6A-D), and increased pH3-immunostaining (Fig. 6C) and BrdU incorporation [14.62±5.79% of cells transfected with pCIG incorporate BrdU ventrally and 19.59±8.03% cells dorsally (n=4). In Gli3A^{HIGH} embryos the proportion is 25.79±1.56% cells ventrally (P<0,0001) and 32.46±5.23% cells dorsally (n=4) (P<0.0001)] (Fig. 6D,E).

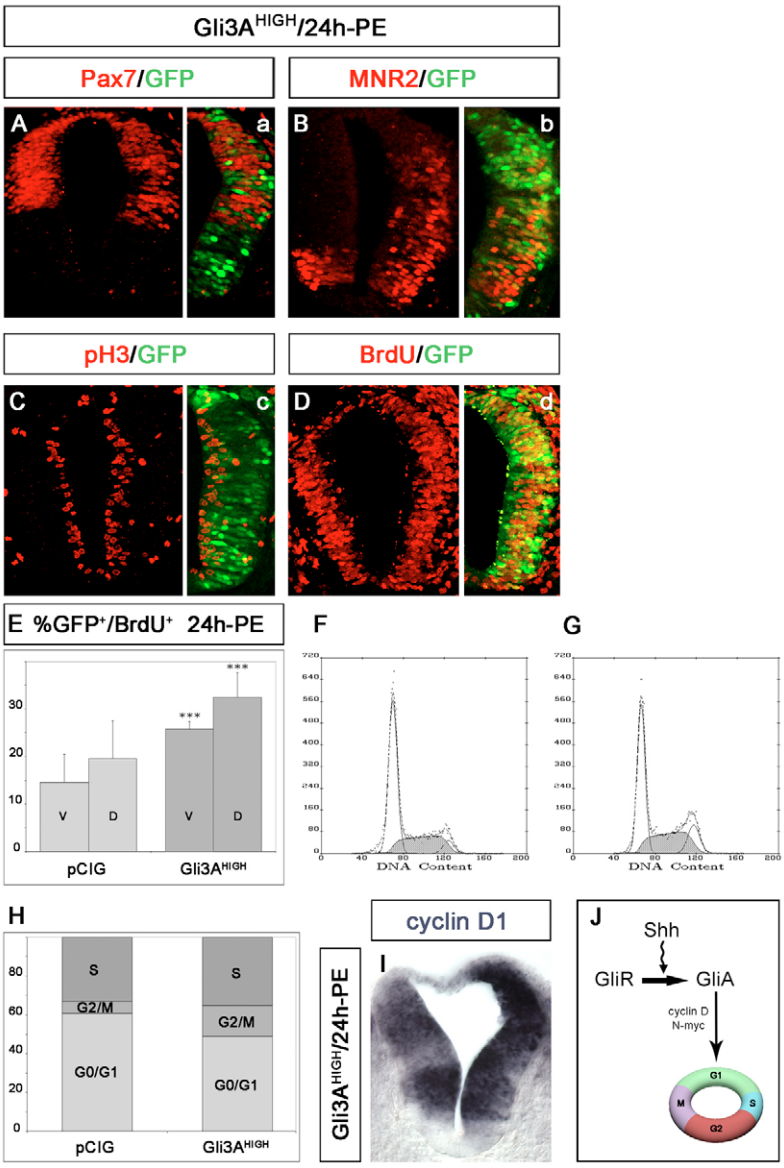

Fig. 6. Gli3A^{HIGH} transfection induces cell fate changes and overproliferation. HH11/12 stage embryos were electroporated with Gli3A^{HIGH} and assayed 24 hours PE for the indicated markers. (**A**,**B**) Electroporation of Gli3A^{HIGH} causes cell-autonomous cell-fate changes, including repression of the dorsal marker Pax7 (A) and activation of the motoneuron marker MNR2 (B). (**C**,**D**) Electroporation of Gli3A^{HIGH} causes overgrowth of the electroporated side, together with increased pH3 staining (C) and increased BrdU incorporation (D). (**E**) Quantitative analysis of Gli3A^{HIGH}/BrdU double-labeled cells in ventral and dorsal neural tubes, after a 1 hour BrdU pulse. At 24 hours PE, the number of cells incorporating BrdU increased ~58% in ventral regions and ~75% in dorsal regions in Gli3A^{HIGH} transfected embryos. Error bars indicate s.d. *P<0.05; **P<0.005; ***P<0.0001 control versus treated. (**F-H**) Flow cytometry analysis of cell cycle phase distribution of transfected cells. pCIG and Gli3A^{HIGH} vectors were electroporated in ovo. At 24 hours PE, neural tubes were dissected out, GFP-expressing cells separated by flow cytometry and cell cycle phases analyzed by Hoescht staining. (F,G) Representative examples of the cell cycle profile of cells expressing pCIG (F) or Gli3A^{HIGH} (G). (H) At 24 hours PE, in Gli3A^{HIGH} transfected embryos there was a ~9% decrease in the number of cells accumulating at G0/G1 phase of the cell cycle. (**I**) In situ hybridization with a chick *cyclin D1* probe in an embryo electroporated with Gli3A^{HIGH}, analyzed 24 hours PE. Electroporated side is to the right. *cyclin D1* expression is upregulated. (**J**) Summary of Shh/Gli activities on cell cycle progression of neuroepithelial cells.

To further examine how transfection of Gli3A^{HIGH} modulated cell cycle phase distribution, neuroepithelial cells electroporated with the control vector pCIG (Fig. 6F) or with Gli3A^{HIGH} (Fig. 6G) were analyzed by flow cytometry. Twenty-four hours PE with pCIG-transfection, 61% of neuroepithelial cells were present in the G1 phase of the cell cycle (1N DNA content), 33% of cells were in the S phase (intermediate DNA content) and 6% of cells were in the G2/M phase (2N DNA content) (Fig. 6H). However, Gli3A transfection decreased the proportion of cells in G1 to 49% and increased the number in S phase to 36% and to 16% cells for in G2/M phase (Fig. 6H). These results support a model in which Gli transcriptional activation shortens the length of G1 for neuroepithelial cells, resulting in a higher proportion of cells residing in S or G2/M at the time of analysis.

Consistent with this idea, transfection of Gli3A^{HIGH} increased the expression of genes involved in progression of the G1 phase of the cell cycle, such as cyclin D1 (Fig. 6I) and N-myc (data not shown) in the neural tube. Thus, both cyclin D1 and N-myc seem to be conserved Gli-transcriptional target genes (Oliver et al., 2003; Kenney and Rowitch, 2002; Kenney et al., 2003; Lobjois et al., 2004).

DISCUSSION

In this study, we provide evidence that Shh signaling regulates, in a cell-autonomous manner, the proliferation and survival of progenitors in the developing neural tube. Moreover, our data indicate that the patterning, mitogenic and survival functions of Shh signaling are discrete activities, separately regulated independent of one another. Nevertheless, the control of each of these properties is mediated by the regulation of Gli activity, suggesting that patterning, growth and survival of neural progenitors is controlled by the transcriptional regulation of discrete sets of target genes.

During neural development, Shh, which is produced by the axial midline structures of the notochord and floor plate (Martí et al., 1995), functions as a long-range signal to direct the dorsoventral patterning of neural progenitors and control neuronal subtype identity (Jessell, 2000; Briscoe and Ericson, 2001). In addition, Shh signaling is required for growth and survival of neural progenitors. We provide evidence that this requirement for Shh signaling is cell-autonomous. Thus, decreases in proliferation observed on blockade of Shh signaling is restricted to those progenitors transfected with the inhibitory constructs (Ptc1$^{\Delta loop2}$ and Gli3R), while increases in proliferation is restricted to cells transfected with the activating constructs (dnPKA and Gli3A^{HIGH}). This indicates a direct influence of Shh on the control of proliferation of cells and, although the data do not exclude the possibility that other factors, in conjunction with Shh signaling, influence the proliferation and survival of progenitors, this study argues against an exclusively indirect role for Shh in which Shh signaling induces the expression of another secreted molecule that acts at long range to promote the growth of the neural progenitors.

Notably, blockade of Shh signaling in both dorsal and ventral regions of the neural tube affects the survival and proliferation of progenitors. One possibility is that a tonic, ligand-independent low-level activation of the pathway in dorsal regions may be sufficient to maintain progenitor proliferation and survival. Alternatively, it is possible that there is an extended range of influence of Shh that includes progenitors throughout most of the neural tube. This would be consistent with the observation that elevated levels of the Shh responsive gene, Ptc1, are present in a broad domain of progenitors that includes the dorsal neural tube (Goodrich et al., 1997). Moreover in embryos lacking Shh signaling (Chiang et al., 1996; Litingtung and Chiang, 2000; Thibert et al., 2003; Wijgerde et al., 2002) the entire neural tube, not just the ventral regions appear decreased in size. Thus, the long-range action of Shh could be required not only for the patterning of progenitors but also for their survival and proliferation, providing a means to couple these attributes of neural cells.

The canonical transduction of Shh signals is initiated by Shh binding to Patched and culminates with the regulation of activity of transcription factors of the Gli family, which control Shh regulated gene expression (reviewed by Jacob and Briscoe, 2003). Although evidence of non-canonical signaling mechanisms has emerged (Thibert et al., 2003; Barnes et al., 2001; Testaz et al., 2001), raising the possibility that the regulation of cell survival and proliferation by Shh precedes via a non canonical pathway independent of Gli activity, our data suggest that this is not the case. Blockade of Shh signaling at either the receptor level, using Ptc1$^{\Delta loop2}$, or at the transcriptional effector level using the dominant inhibitory Gli protein Gli3R had similar effects: promoting apoptosis and decreasing proliferation. Moreover, the pro-apoptotic and anti-mitogenic activity of Ptc1$^{\Delta loop2}$ could be counteracted by the simultaneous transfection of a dominant-active Gli protein, Gli3A^{HIGH}, suggesting that Gli activity is epistatic to Ptc1. The anti-proliferative effect of Ptc1$^{\Delta loop2}$ was also blocked by co-expression of Gli-ZnF, a construct consisting only of the DNA-binding domain of Gli3 that is capable of blocking both the repressor and activator functions of Gli. This suggests that in Ptc1$^{\Delta loop2}$-expressing cells, it is the increase in Gli repressor activity that is responsible for the reduced proliferation rate. By contrast, the expression of Gli-ZnF alone promoted apoptosis in neural cells. This level of apoptosis was not increased by the co-expression of Ptc1$^{\Delta loop2}$ with Gli-ZnF, as would be expected if the two proteins induced apoptosis via distinct pathways. Rather, the proapoptotic effect of Gli-ZnF suggests that a tonic level of Gli activator protein is required for the survival of neuroepithelial cells. Titration of this activator protein either using Gli-ZnF or by expression of Ptc1$^{\Delta loop2}$ can decrease the survival of neuroepithelial cells.

Consistent with these data, the growth defects observed in the neural tubes of mouse embryos lacking Shh or Smo are rescued in double mutant embryos that also lack Gli3, suggesting that, in the absence of Shh signaling, Gli3 functions to repress proliferation and cell survival (Litingtung and Chiang, 2000). Inhibition of the repressive activity of Gli3 either by increasing Shh signaling or genetic removal of Gli3 relieves this repression, allowing progenitors to survive and grow. Together with the data presented here, therefore, the evidence supports a central role for the regulation of Gli activity in the control of neural cell proliferation and survival. What contributions non-canonical mechanisms make to the control of these properties and whether these non-canonical pathways ultimately converge on the regulation of Gli activity remain to be determined.

Our data suggest that the regulation of cell survival and proliferation by Shh are independent of one another. Inhibition of Shh signaling by Ptc1$^{\Delta loop2}$ results in decreases in the proliferation rate of neural cells prior to the onset of apoptosis. Thus, delayed apoptosis could be interpreted as a consequence of cell cycle arrest and the induction of ‘mitotic collapse’. However, several lines of evidence argue against this. First, the expression of Gli-ZnF promotes apoptosis without affecting the proliferation rate of neuroepithelial cells. Second, the expression of Gli3R is able to induce high levels of apoptosis within 6 hours of transfection, prior to any detectable change in proliferation, suggesting a direct effect on a gene or genes necessary for the survival of neuroepithelial

cells. Thus, the decrease in cell survival in the absence of Shh signaling does not appear to be exclusively a consequence of cell cycle arrest; instead, the data suggest that Shh signaling directly regulates cell survival, independently of proliferation rate. Conversely, ectopic activation of Shh signaling with Gli3A^{HIGH} increases the rate of proliferation without affecting the survival of neural cells. Moreover, a decrease in mitogenesis is also observed in cells unable to respond to Shh in which apoptosis has been blocked by forced expression of Bcl2. Together these data suggest that the lower levels of proliferation observed on blockade of Shh signaling are not a simply a consequence of an increase in apoptosis, but instead a consequence of Gli mediated regulation of cell cycle progression.

Previous studies have suggested that canonical Wnt signaling from the dorsal aspect of the neural tube via activation of β-catenin has an important role in the control of precursor cell proliferation (Megason and McMahon, 2002). The data showing that Shh also influences the proliferation and survival of neural progenitors raise the issue of how these two mitogenic factors interact to ensure the normal growth of progenitors. It is possible that the two factors regulate the growth of the neural tube via distinct mechanisms involving different transcriptional responses. Alternatively, it is possible that both factors converge on the same set of target genes; indeed, the possibility of cross-talk between the two should not be ruled out given the number of shared components between the two pathways (Meng et al., 2001; Jia et al., 2002; Price and Kalderon, 2002) and the number of common target genes (Megason and McMahon, 2002; Panhuysen et al., 2004). Accordingly, cross-talk between the two pathways may act to integrate the mitogenic and survival responses of cells to ensure the well regulated growth and morphogenesis of the neural tube.

The identity of the target genes that control the survival and proliferation of neural progenitors remains to be clarified. The regulation of dorsoventral position by Shh signaling involves a group of transcription factors that control neuronal subtype identity by partitioning neural progenitors into a series of domains (Jessell, 2000; Briscoe and Ericson, 2001). These transcription factors do not, however, appear to be involved in the regulation of the proliferation or survival of progenitors. There are no reported changes in the growth or survival of neural progenitors in gain- or loss-of-function experiments that change the expression of the homeodomain proteins (Briscoe et al., 2000; Ericson et al., 1997; Muhr et al., 2001; Novitch et al., 2001; Pierani et al., 2001; Vallstedt et al., 2001), despite their ability to change the dorsoventral organization of the neural tube and the pattern of neuronal subtype generation. Moreover, in the current study, we provide evidence that the changes in the proliferation rate and survival of cells elicited by the blockade of Shh signaling occur rapidly, prior to evident changes in the expression of homeodomain protein expression. Indeed, Gli3R appears to induce high levels of neural apoptosis within 6 hours of transfection, precluding the presence of multiple steps between Gli repression and a proapoptotic response. Furthermore, activated Gli constructs that mimic different levels of Shh signaling and induce different sets of homeodomain proteins (Stamataki et al., 2005) have similar effects on promoting the proliferation of progenitors (data not shown). Together, these data dissociate the expression of the transcription factors that pattern progenitors from the control of neural progenitor survival and proliferation, raising the possibility that Gli activity may directly regulate the genes that mediate these distinct responses.

A number of candidate genes have been previously identified as Shh responsive and involved in cell survival and advancing the cell cycle. Bcl2 is induced in keratinocytes (Bigelow et al., 2004; Regl et al., 2004) and we demonstrate an upregulation of Bcl2 in neural cells expressing an activated Gli construct, thus the regulation of Bcl2 may ensure the survival of neural progenitors. Our analysis of the cell cycle indicates that Shh signaling affects the length of G1, consistent with this idea N-myc (Kenney et al., 2003) and cyclin D1 (Oliver et al., 2003; Kenney and Rowitch, 2002; Lobjois et al., 2004) have been found to be responsive to Shh signaling in the developing cerebellum and in the neural tube. Indeed our analysis indicates that alteration of Shh signaling in the neural tube affects the expression of both N-myc and cyclin D1; however, the changes in the expression of these two genes does not appear to be sufficient to account for the observed changes in the cell cycle. For example, Gli3R expression represses the ventral expression of cyclin D1; however, cyclin D1 expression is maintained in dorsal progenitors, despite the proliferation rate of these cells being retarded to the same extent as ventral progenitors. Conversely, the expression of N-myc is observed in intermediate and dorsal progenitors but is excluded from ventral regions, suggesting that other genes must promote proliferation ventrally. Other candidates for affecting the proliferation of neural progenitors include genes such as the polycomb group protein Bmi1 (Leung et al., 2004). Identifying the genes regulated by Shh signaling that mediate the proliferative responses and survival of neural cells may shed light on how Shh signaling coordinates progenitor growth and survival with the patterning of the neural tube and cell fate specification.

We thank Susana Usieto for invaluable research assistance, Jaume Comas for skilled assistance with the FACS, Rubén Alvarez for help on western blots and Gemma Martí for illustrations. Monoclonal antibodies to, Pax7, islet 1 (40.2D6), Mnr2 (81.5C10) and Nkx2.2 (74.5A5) were all obtained from the Developmental Studies Hybridoma Bank, developed under the auspices of the NICHD and maintained by The University of Iowa, Department of Biological Sciences, Iowa City, IA 52242. Work in E.M.'s laboratory is supported by the Spanish Ministry of Education Grant BFU2004-00455/BMC and by the EU BioTech-Grant QLRT-2002-01141, which also supported J.C. Work in J.B.'s laboratory is supported by MRC (UK). F.U. is supported by an EMBO LTF. B.C. is supported by EU BioTech-Grant QLRT-2002-01141.

Supplementary material

Supplementary material for this article is available at
http://dev.biologists.org/cgi/content/full/133/3/517/DC1

References

Bai, C. B., Stephen, D. and Joyner, A. L. (2004). All mouse ventral spinal cord patterning by hedgehog is Gli dependent and involves an activator function of Gli3. *Dev. Cell* **6**, 103-115.

Barnes, E. A., Kong, M., Ollendorff, V. and Donoghue, D. J. (2001). Patched1 interacts with cyclin B1 to regulate cell cycle progression. *EMBO J.* **20**, 2214-2223.

Bastida, M. F., Delgado, M. D., Wang, B., Fallon, J. F., Fernandez-Terán, M. and Ros, M. A. (2004). Levels of Gli3 repressor correlate with Bmp4 expression and apoptosis during limb development. *Dev. Dyn.* **231**, 148-160.

Bigelow, R. L. H., Chari, N. S., Unden, A. B., Spurgers, K. B., Lee, S., Roop, D. R., Toftgard, R. and McDonnell, T. J. (2004). Transcriptional regulation of bcl-2 mediated by the Sonic hedgehog signalling pathway through gli-1. *J. Biol. Chem.* **279**, 1197-1205.

Briscoe, J. and Ericson, J. (2001). Specification of neuronal fates in the ventral neural tube. *Curr. Opin. Neurobiol.* **11**, 43-49.

Briscoe, J., Pierani, A., Jessell, T. M. and Ericson, J. (2000). A homeodomain protein code specifies progenitor cell identity and neuronal fate in the ventral neural tube. *Cell* **101**, 435-445.

Briscoe, J., Chen, Y., Jessell, T. M. and Struhl, G. (2001). A hedgehog-insensitive form of Patched provides evidence for the direct long range morphogen activity of Sonic hedgehog in the neural tube. *Mol. Cell* **7**, 1279-1291.

Charrier, J. B., Lapointe, F., LeDouarin, N. M. and Teillet, A. M. (2001). Anti-apoptotic role of Sonic hedgehog protein at the early stages of nervous system organogenesis. *Development* **128**, 4011-4020.

Chiang, C., Litingtung, Y., Lee, E., Young, K. E., Corden, J. L., Westphal, H.

and Beachy, P. A. (1996). Cyclopia and defective axial patterning in mice lacking Sonic hedgehog gene function. *Nature* **383**, 407-413.
Dahmane, N. and Ruiz i Altaba, A. (1999). Sonic hedgehog regulates the growth and patterning of the cerebellum. *Development* **126**, 3089-3100.
Dahmane, N., Sanchez, P., Gitton, Y., Palma, V., Sun, T., Beyna, M., Weiner, H. and Ruiz i Altaba, A. (2001). The Sonic Hedgehog-Gli pathway regulates dorsal brain growth and tumorigenesis. *Development* **128**, 5201-5212.
Dickinson, M. E., Krumlauf, R. and McMahon, A. P. (1994). Evidence for a mitogenic effect of Wnt-1 in the developing mammalian central nervous system. *Development* **120**, 1453-1471.
Epstein, D. J., Martí, E., Scott, M. P. and McMahon, A. (1996). Antagonizing cAMP-dependent protein kinase A in the dorsal CNS activates a conserved Sonic hedgehog signaling pathway. *Development* **122**, 2885-2894.
Ericson, J., Rashbass, P., Schedl, A., Brenner-Morton, S., Kawakami, A., van Heyningen, V., Jessell, T. M. and Briscoe, J. (1997). Pax6 controls progenitor cell identity and neuronal fate in response to graded Shh signaling. *Cell* **90**, 169-180.
Goodrich, L. V., Milenkovic, L., Higgins, K. M and Scott, M. P. (1997). Altered neural cell fates and medulloblastoma in mouse patched mutants. *Science* **277**, 1109-1113.
Hamburger, V. and Hamilton, H. L. (1951). A series of normal stages in the development of chick embryo. *J. Morphol*. **88**, 49-92.
Helms, A. W. and Johnson, J. E. (2003). Specification of dorsal spinal cord interneurons. *Curr. Opin. Neurobiol.* **13**, 42-49.
Hynes, M., Ye, W., Wang, K., Stone, D., Murone, M., Sauvage, F. and Rosenthal, A. (2000). The seven-transmembrane receptor smoothened cell-autonomously induces multiple ventral cell types. *Nat. Neurosci*. **3**, 41-46.
Jacob, J. and Briscoe, J. (2003). Gli proteins and the control of spinal-cord patterning. *EMBO Rep.* **8**, 761-765.
Jeong, J. and McMahon, A. P. (2005). Growth and pattern of the mammalian neural tube are governed by partially overlapping feedback activities of the hedgehog antagonists patched1 and Hhip1. *Development* **132**, 143-154.
Jessell, T. M. (2000). Neuronal specification in the spinal cord: inductive signals and transcriptional codes. *Nat. Rev. Genet*. **1**, 20-29.
Jia, J., Amanai, K., Wang, G., Tang, J., Wang, B. and Jiang, J. (2002). Shaggy/GSK3 antagonizes Hedgehog signalling by regulating Cubitus interruptus. *Nature* **416**, 548-552.
Kenney, A. M. and Rowitch, D. H. (2002). Sonic hedgehog promotes G1 Cyclin expression and sustained cell cycle progression in mammalian neuronal precursors. *Mol.Cell Biol*. **20**, 9055-9067.
Kenney, A. M., Cole, M. D., Rowitch, D. H. (2003). Nmyc upregulation by sonic hedgehog signalling promotes proliferation in developing cerebellar granule neuron precursors. *Development* **130**, 15-20.
Lai, K., Kaspar, B. K., Gage, F. H. and Schaffer, D. V. (2003). Sonic hedgehog regulates adult neural progenitor proliferation in vitro and in vivo. *Nat. Neurosci*. **6**, 21-27.
Lei, Q., Zelman, A. K., Kuang, E., Li, S. and Matise, M. P. (2004). Transduction of graded Hedgehog signaling by a combination of Gli2 and Gli3 activator functions in the developing spinal cord. *Development* **131**, 3593-3604.
Leung, C., Lingbeek, M., Shakhova, O., Liu, J., Tanger, E., Saremaslani, P., Van Lohuizen, M. and Marino, S. (2004). Bmi1 is essential for cerebellar development and is overexpressed in human medulloblastomas. *Nature* **428**, 337-341.
Litingtung, Y. and Chiang, C. (2000). Specification of ventral neuron types is mediated by an antagonistic interaction between Shh and Gli3. *Nat. Neurosci*. **10**, 979-985.
Lobjois, V., Benazeraf, B., Bertrand, N., Medevielle, F. and Pituello, F. (2004). Specific regulation of cyclins D1 and D2 by FGF and Shh signaling coordinates cell cycle progression, patterning and differentiation during early steps of spinal cord development. *Dev. Biol.* **273**, 195-209.
Lum, L. and Beachy, P. A. (2004). The Hedgehog response network: sensors, switches, and routers. *Science* **304**, 1755-1759.
Machold, R., Hayashi, S. M., Muzumdar, M. D., Nery, S., Corbin, J. G., Gritli-Linde, A., Dellovade, T., Porter, J. A., Rubin, L. L., Dudek, H, McMahon, A. P. and Fishell, G. (2003). Sonic hedgehog is required for progenitor cell maintenance in telencephalic stem cell niches. *Neuron* **39**, 937-950.
Martí, E., Takada, R., Bumcrot, D. A., Sasaki, H. and McMahon, A. P. (1995). Distribution of Sonic hedgehog peptides in the developing chick and mouse embryo. *Development* **120**, 2537-2547.
Megason, S. and McMahon, A. P. (2002). A mitogen gradient of dorsal midline Wnts organizes growth in the CNS. *Development* **129**, 2087-2098.
Meng, X., Poon, R., Zhang, X., Cheah, A., Ding, Q., Hui, C. C. and Alman, B. (2001). Suppressor of fused negatively regulates beta-catenin signaling. *J. Biol. Chem.* **276**, 40113-40119.
Meyer, N. P. and Roelink, H. (2003). The amino-terminal region of Gli3 antagonizes the Shh response and acts in dorsoventral fate specification in the developing spinal cord. *Dev. Biol*. **257**, 343-355.
Muhr, J., Andersson, E., Persson, M., Jessell, T. M. and Ericson, J. (2001). Groucho-mediated transcriptional repression establishes progenitor cell pattern and neuronal fate in the ventral neural tube. *Cell* **104**, 861-873.
Niwa, H., Yamamura, K. and Miyazaki, J. (1991). Efficient selection for high expression transfectants with as novel eukaryotic vector. *Gene* **15**, 193-199.
Novitch, B. G., Chen, A. I. and Jessell, T. M. (2001). Coordinate regulation of motor neuron subtype identity and pan-neuronal properties by the bHLH repressor Olig2. *Neuron* **31**, 773-789.
Oliver, T. G., Grasfeder, L. L., Carroll, A. L., Kaiser, C., Gillingham, C. L., Lin, S. M., Wickramasinghe, R., Scott, M. P. and Wechsler-Reya, R. J. (2003). Transcriptional profiling of the Sonic hedgehog response: a critical role for N-myc in proliferation of neuronal precursors. *Proc. Natl. Acad. Sci. USA* **100**, 7331-7336.
Palma, V. and Ruiz i Altaba, A. (2004). Hedgehog-GLI signaling regulates the behaviour of cells with stem cell properties in the developing neocortex. *Development* **131**, 337-345.
Panhuysen, M., Vogt Weisenhorn, D. M., Blanquet, V., Brodski, C., Heinzmenn, U., Beisker, W. and Wurst, W. (2004). Effects of Wnt1 signaling on proliferation in the developing mid-/hindbrain region. *Mol. Cell Neurosci*. **26**, 101-111.
Persson, M., Stamataki, D., Welscher, P., Anderson, E., Bose, J., Ruther, U., Ericson, J. and Briscoe, J. (2002). Dorsal-ventral patterning of the spinal cord requires Gli3 transcriptional repressor activity. *Genes Dev*. **16**, 2865-2878.
Pierani, A., Moran-Rivard, L., Sunshine, M. J., Littman, D. R., Goulding, M. and Jessell, T. M. (2001). Control of interneuron fate in the developing spinal cord by the progenitor homeodomain protein Dbx1. *Neuron* **29**, 367-384.
Placzek, M., Jessell, T. M. and Dodd, J. (1993). Induction of floor plate differentiation by contact-dependent, homeogenetic signals. *Development* **117**, 205-218.
Pons, S., Trejo, J. L., Martínez-Morales, J. R. and Martí, E. (2001). Vitronectin regulates Sonic hedgehog activity during cerebellum development through CREB phosphorylation. *Development* **128**, 1481-1492.
Price, MA and Kalderon, D. (2002). Proteolysis of the Hedgehog signaling effector Cubitus interruptus requires phosphorylation by Glycogen Synthase Kinase 3 and Casein Kinase 1. *Cell* **108**, 823-835.
Ramón y Cajal, S. (1911). *Histologie du Sisteme Nerveux de l'Homme et des Vertebrates.* Paris: Malonie.
Regl, G., Kasper, M., Schnidar, H., Eichberger, T., Neill, G. W., Philpott, M. P., Esterbauer, H., Hauser-Kronberger, C., Frischauf, A. M. and Aberger, F. (2004). Activation of the BCL2 promoter in response to Hedgehog/GLI signal transduction is predominantly mediated by GLI2. *Cancer Res*. **64**, 7724-7731.
Rowitch, D. H., S-Jacques, B., Lee, S. M., Flax, J. D., Snyder, E. Y. and McMahon, A. P. (1999). Sonic hedgehog regulates proliferation and inhibits differentiation of CNS precursor cells. *J. Neurosci*. **19**, 8954-8965.
Stamataki, D., Ulloa, F., Tsoni, S. V., Mynnett, A. and Briscoe, J. (2005). A gradient of Gli activity mediates graded Sonic hedgehog signalling in the neural tube. *Genes Dev.* **19**, 626-641.
Testaz, S., Jarov, A., Williams, K. P., Ling, L. E., Koteliansky, V. E., Fournier-Thibault, C. and Duband, J. L. (2001). Sonic hedgehog restricts adhesion and migration of neural crest cells independently of the Patched- Smoothened-Gli signaling pathway. *Proc. Natl. Acad. Sci. USA* **98**, 12521-12526.
Thibert, C., Teillet, M.-A., Lapointe, F., Mazelin, L., LeDouarin, N. M. and Mehlen, P. (2003). Inhibition of neuroepithelial patched-induced apoptosis by Sonic hedgehog. *Science* **301**, 843-846.
Vallstedt, A., Muhr, J., Pattyn, A., Pierani, A., Mendelsohn, M., Sander, M., Jessell, T. M. and Ericson, J. (2001). Different levels of repressor activity assign redundant and specific roles to Nkx6 genes in motor neuron and interneuron specification. *Neuron* **31**, 743-755.
van Straaten, H. W. and Hekking, J. W. (1991). Development of the floorplate, neurons and axonal outgrowth pattern in the early spinal cord of the notochord-deficient chick embryos. *Anat. Embryol.* **184**, 55-63.
van Straaten, H. W., Hekking, J. W., Beursgens, J. P., Terwindt-Rouwenhorst, E. and Drukker, J. (1989). Effect of the notochord on proliferation and differentiation in the neural tube of the chick embryo. *Development* **107**, 793-803.
Wallace, V. A. (1999). Purkinje-cell-derived Sonic hedgehog regulates granule neurone precursor cell proliferation in the developing mouse cerebellum. *Curr. Biol*. **9**, 445-448.
Wang, B., Fallon, J. F. and Beachy, P. A. (2000). Hedgehog regulated processing of Gli3 produces and anterior-posterior repressor gradient in the developing vertebrate limb. *Cell* **100**, 423-434.
Wechsler-Reya, R. J. and Scott, M. P. (1999). Control of neuronal precursor proliferation in the cerebellum by sonic hedgehog. *Neuron* **22**, 103-114.
Wijgerde, M., McMahon, J., Rule, M. and McMahon, A. P. (2002). A direct requirement for Hedgehog signaling for normal specification of all ventral progenitor domains in the presumptive mammalian spinal cord. *Genes Dev.* **16**, 2849-2864.